EFFECT OF JOULE HEATING AND HALL CURRENT ON MHD FLOW OF A NANOFLUID DUE TO A ROTATING DISK WITH VISCOUS DISSIPATION

by

***Mohamed S. ABDEL-WAHED*[a*] *and Tarek G. EMAM*[b,c]**

[a] Basic Sciences Department, Faculty of Engineering at Benha, Benha University, Cairo, Egypt
[b] Department of Mathematics, Faculty of Science, Ain Shams University, Abbassia, Cairo, Egypt
[c] Department of Mathematics, Faculty of Science and Arts, Khulais, University of Jeddah, Jeddah, Saudi Arabia.

Original scientific paper
https://doi.org/10.2298/TSCI160312218A

The present work provides an analysis of the hydromagnetic nanofluid boundary-layer flow over a rotating disk in a porous medium with a constant velocity in the presence of hall current and thermal radiation. The governing PDE system that describes the problem is converted to a system of ODE by the similarity transformation method, which solved analytically using optimal homotopy asymptotic method. The velocity profiles and temperature profiles of the boundary-layer are plotted and investigated in details. Moreover, the surface skin friction, rate of heat transfer are deduced and explained in details.

Key words: *nanofluids, Hall current, magnetic field, joule heating, thermal radiation, viscous dissipation*

Introduction

The problem of rotating disk in a fluid has attracted the attention of many researchers for its applications in industry such as manufacturing and using computer disks, crystal growth processes, rotating viscometer, rotating machines, *etc.* The classical problem of rotating disk was investigated by Von Karman [1], He has reduced the Navier-Stokes equations for steady flow to a set of ODE. Such equations can be solved using an approximate integral method. Such results were further improved by Cochran [2], Benton [3], and Rogers and Lance [4] they extended the problem to the flow starting impulsively from rest. Edrogan [5] has analyzed the unsteady fluid flow by non-coaxial rotations of a disk and a fluid at infinity. Turkyilmazoglu [6] extended the work of them by considering a magnetic field. While Sheikholeslami *et al.* [7] studied the nanofluid flow and heat transfer due to a rotating disk. Elbashbeshy and Eman [8] have studied the effect of thermal radiation and heat transfer over an unsteady stretching sheet. Recently Hayat *et al.* [9] have studied the MHD steady flow of viscous nanofluid due to a rotating disk with partial slip.

A nanofluid is fluid in which solid nanoparticles with the length scales of 1-100 nm are suspended in conventional heat transfer basic fluid. Such Nanoparticles enhance thermal conductivity and convective heat transfer coefficient of the base fluid significantly. Nanofluids plays an important role in rising thermal conductivity of many fluids which have already

* Corresponding author, e-mail: eng_moh_sayed@live.com

low thermal conductivity such as water, ethylene glycol, oil, *etc.* Choi and Eastman [10] have firstly used the nanoparticles to enhance thermal conductivity of fluids and heat transfer rate. Nanofluids have very important industrial applications. Such fluids used to increase the heat transfer rate of microelectronics and microchips in computer devices. The study of MHD flow has many physical applications as well as industrial applications such as generators and pumps. The interaction between the electrically conducting fluid and magnetic field affects the boundary-layer flow. The MHD layers observed in many technical systems employing liquid metal and plasma flow transverse of magnetic fields. Liron *et al.* [11] deduced a solution for the MHD boundary-layer equations using Meksyn's method. Elbashbeshy *et al.* [12, 13] investigate the effect of thermal radiation on the nanofluid boundary-layer over a moving cylinder and non-flat moving surface, respectively. Makinde *et al.* [14] studied the MHD flow of variable viscosity nanofluid over a stretching surface. Khamis *et al.* [15] studied the unsteady MHD flow of variable viscosity nanofluid in a porous pipe with buoyancy. Makinde *et al.* [16] studied the effect of viscous dissipation and Newtonian heating on boundary-layer flow of nanofluids over a flat plate. Motsumi *et al.* [17] studied effects of thermal radiation and viscous dissipation on boundary-layer flow of nanofluids over a permeable moving flat plate. Rashidi *et al.* [18] studied the entropy generation in steady MHD flow due to a rotating porous disk in a nanofluid. The hall current effect on the MHD boundary-layer and the viscous dissipation studied by Chauhan *et al.* [19], Babaelhi *et al.* [20], and Sheikholeslami [21],

The present study discusses the effect of thermal radiation on the MHD boundary-layer over a rotating disk in the presence of hall current and joule heating. The governing boundary-layer equations transformed to a system of non-linear-coupled equations and solved by the optimal homotopy technique [22, 23].

Formulation of the problem

Consider a steady-laminar flow of an electrically conducting nanofluid with hall current effect induced by a non-conducting rotating disk at $z = 0$. The disk rotates with constant angular velocity, Ω, about the z-axis. Fluid is assumed to fill the porous medium. Components of the flow velocity are (u, v, w) in the direction of increasing (r, φ, z), respectively. Consider also that a uniform magnetic field of strength, B_o, is applied normal to the plane of the disk. Thermal radiation with heat flux, q_r, is taken into consideration. The surface of the rotating disk has uniform temperature, T_w, while temperature far away from the surface is T_∞, fig. 1.

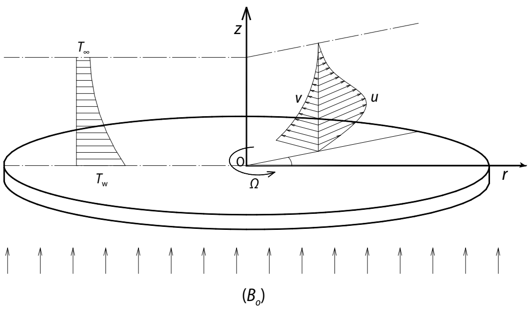

Figure 1. Physical model and co-ordinate system

$$\frac{\partial u}{\partial r}+\frac{u}{r}+\frac{\partial w}{\partial z}=0 \tag{1}$$

$$\rho_{\text{nf}}\left(u\frac{\partial u}{\partial r}-\frac{v^2}{r}+w\frac{\partial u}{\partial z}\right)+\frac{\partial p}{\partial r}=\mu_{\text{nf}}\left(\frac{\partial^2 u}{\partial r^2}+\frac{1}{r}\frac{\partial u}{\partial r}-\frac{u}{r^2}+\frac{\partial^2 u}{\partial z^2}\right)-\frac{\mu_{\text{nf}}}{K}u-\frac{\sigma_{\text{nf}}\,B_0^{\,2}}{\left(1+m^2\right)}\left(u-mv\right) \tag{2}$$

$$\rho_{\mathrm{nf}}\left(u\frac{\partial v}{\partial r}+\frac{uv}{r}+w\frac{\partial v}{\partial z}\right)=\mu_{\mathrm{nf}}\left(\frac{\partial^2 v}{\partial r^2}+\frac{1}{r}\frac{\partial v}{\partial r}-\frac{v}{r^2}+\frac{\partial^2 v}{\partial z^2}\right)-\frac{\mu_{\mathrm{nf}}}{K}v-\frac{\sigma_{\mathrm{nf}}B_0^{\ 2}}{\left(1+m^2\right)}\left(v+mu\right) \tag{3}$$

$$\rho_{\mathrm{nf}}\left(u\frac{\partial w}{\partial r}+w\frac{\partial w}{\partial z}\right)+\frac{\partial p}{\partial z}=\mu_{\mathrm{nf}}\left(\frac{\partial^2 w}{\partial r^2}+\frac{1}{r}\frac{\partial w}{\partial r}+\frac{\partial^2 w}{\partial z^2}\right)-\frac{\mu_{\mathrm{nf}}}{K}w \tag{4}$$

$$(\rho C_p)_{\mathrm{nf}}\left(u\frac{\partial T}{\partial r}+w\frac{\partial T}{\partial z}\right)=k_{\mathrm{nf}}\left(\frac{\partial^2 T}{\partial r^2}+\frac{1}{r}\frac{\partial T}{\partial r}+\frac{\partial^2 T}{\partial z^2}\right)+\sigma_{\mathrm{nf}}B_0^2\left(u^2+v^2\right)+$$
$$+\mu_{\mathrm{nf}}\left\{2\left[\left(\frac{\partial u}{\partial r}\right)^2+\left(\frac{u}{r}\right)^2+\left(\frac{\partial w}{\partial z}\right)^2\right]+\left(\frac{\partial u}{\partial z}+\frac{\partial w}{\partial r}\right)^2+\left(\frac{\partial v}{\partial r}-\frac{v}{r}\right)^2\right\}-\frac{\partial q_r}{\partial z} \tag{5}$$

where ρ_{nf} is the nanofluid density, μ_{nf} – the nanofluid viscosity, σ_{nf} – the electrical conductivity of nanofluid, K – the permeability of the porous medium, tab. 1, m is the Hall current parameter ($m = \tau_e\,\omega_e$), where τ_e – the electron collusion time and ω_e – cyclotron frequency, p – the pressure, k_{nf} – the thermal conductivity, and $(\rho C_p)_{\mathrm{nf}}$ – the specific heat capacity.

Table 1. Thermophysical properties of water and the elements CuO and Al_2O_3 [9]

Properties	Fluid (water)	CuO	Al_2O_3
C_p [Jkg^{-1}K^{-1}]	4179	540	765
ρ [kgm^{-3}]	997.1	6500	3970
k [Wm^{-1}K^{-1}]	0.613	18	25
σ [Ωm^{-1}]	0.05	10^{-10}	10^{-12}

The boundary conditions for the previous described model are:

$$u=0,\quad v=\Omega r,\quad w=0,\quad T=T_w \quad \text{at} \quad z=0 \tag{6}$$

$$u\to 0,\quad v\to 0,\quad T=T_\infty,\quad P=P_\infty \quad \text{as} \quad z\to\infty \tag{7}$$

The properties of nanofluid defined [9]:

$$\mu_{\mathrm{nf}}=\frac{\mu_{\mathrm{f}}}{(1-\phi)^{2.5}},\quad \rho_{\mathrm{nf}}=(1-\phi)\rho_{\mathrm{f}}+\phi\rho_{\mathrm{s}},\quad (\rho C_p)_{\mathrm{nf}}=(\rho C_p)_{\mathrm{f}}(1-\phi)+\phi(\rho C_p)_{\mathrm{s}}$$

$$\frac{\sigma_{\mathrm{nf}}}{\sigma_{\mathrm{f}}}=1+\frac{3\phi\left(\dfrac{\sigma_{\mathrm{s}}}{\sigma_{\mathrm{f}}}-1\right)}{\left(\dfrac{\sigma_{\mathrm{s}}}{\sigma_{\mathrm{f}}}+2\right)-\phi\left(\dfrac{\sigma_{\mathrm{s}}}{\sigma_{\mathrm{f}}}-1\right)},\quad \frac{k_{\mathrm{nf}}}{k_{\mathrm{f}}}=\frac{(k_{\mathrm{s}}+2k_{\mathrm{f}})-2\phi(k_{\mathrm{s}}-k_{\mathrm{f}})}{(k_{\mathrm{s}}+2k_{\mathrm{f}})+\phi(k_{\mathrm{s}}-k_{\mathrm{f}})}$$

where ϕ is the solid volume fraction, subscript, s, is for nano-solid-particles, and subscript, f, is for base fluid.

The fluid is considered to be gray, absorbing-emitting radiation but non-scattering medium and the Rosseland approximation is used to describe the radiative heat flux in the energy equation. By using Rosseland approximation for radiation radiative heat flux is simplified as:

$$q_r=-\frac{4\sigma^*}{3\alpha^*}\frac{\partial T^4}{\partial z} \tag{8}$$

where σ^* and α^* are the Stefen-Boltzman constant and the mean absorption coefficient, respectively. Assuming that the temperature differences within the flow are such that the term T^4 may be expressed as a linear function of temperature and expanding T^4 in a Taylor series about T_∞ while higher order terms are neglected we get:

$$T^4 \cong 4T T_\infty^3 - 3T_\infty^4 \tag{9}$$

Similarity transformations

We look for a similarity solution of eqs. (1)-(5) subjected to the boundary conditions (6) and (7) of the following form:

$$\left\{\begin{matrix} u = r\Omega f', \quad v = r\Omega g, \quad w = -\sqrt{2\Omega\nu_\mathrm{f}}\, f, \quad \theta(\eta) = \dfrac{T - T_\infty}{T - T_w}, \\ P = P_\infty + 2\Omega\mu_\mathrm{f} P(\eta), \quad \eta = \sqrt{\dfrac{2\Omega}{\nu_\mathrm{f}}} z \end{matrix}\right\} \tag{10}$$

where η is the similarity variable. Substitute eq. (8) into eqs. (2)-(5), the following system of non-linear ODE is obtained in the form:

$$2f''' + \left(\frac{A_1}{A_4}\right)\left[2ff'' - f'^2 + g^2\right] - \left(\frac{A_5}{A_4}\right)\frac{\mathrm{M}}{\left(1+m^2\right)}\left(f' - mg\right) - \lambda f' = 0 \tag{11}$$

$$2g'' + \left(\frac{A_1}{A_4}\right)\left[2fg' - 2f'g\right] - \left(\frac{A_5}{A_4}\right)\frac{\mathrm{M}}{\left(1+m^2\right)}\left(g + mf'\right) - \lambda g = 0 \tag{12}$$

$$\theta''\left(1 + \frac{4R_d}{3}\right) + \mathrm{Pr}\left(\frac{A_2}{A_3}\right)f\theta' + \mathrm{Pr\,Ec}\left(\frac{A_4}{A_3}\right)\left[f''^2 + \left(\frac{6}{\mathrm{Re}}\right)f'^2\right] + \mathrm{Pr\,Ec\,M}\left(\frac{A_5}{A_3}\right)\left[f'^2 + g^2\right] = 0 \tag{13}$$

where the prime denotes differentiation with respect to η and:

$$A_1 = \frac{\rho_\mathrm{nf}}{\rho_\mathrm{f}}, \quad A_2 = \frac{(\rho C_p)_\mathrm{nf}}{(\rho C_p)_\mathrm{f}}, \quad A_3 = \frac{k_\mathrm{nf}}{k_\mathrm{f}}, \quad A_4 = \frac{\mu_\mathrm{nf}}{\mu_\mathrm{f}}, \quad \text{and} \quad A_5 = \frac{\sigma_\mathrm{nf}}{\sigma_\mathrm{f}}$$

The transformed boundary conditions of the problem are:

$$f(0) = 0, \quad f' = 0, \quad g(0) = 1, \quad \theta(0) = 1 \tag{14}$$

$$f'(\infty) = 0, \quad g(\infty) = 0, \quad \theta(\infty) = 0 \tag{15}$$

where $\mathrm{Pr} = \nu_\mathrm{f}(\rho C_p)_\mathrm{f}/k_\mathrm{f}$ is the Prandtl number, $\lambda = \nu_\mathrm{f}/\Omega k_\mathrm{f}$ – the porosity parameter, $\mathrm{M} = \sigma_\mathrm{f} B_0^2/\Omega\rho_\mathrm{f}$ – the Hartmann number, $\mathrm{Ec} = \rho_\mathrm{f} r^2\Omega^2/(\rho C_p)_\mathrm{f}(T_\mathrm{w} - T_\infty)$ – the Eckert number, $\mathrm{Re} = r^2\Omega/\nu_\mathrm{f}$ – the Reynold number, and $R_d = 4\sigma^* T_\infty^3/k_\mathrm{nf}k^*$ – the radiation parameter.

Analytical solution using optimal homotopy asymptotic method

In this section, the optimal homotopy asymptotic method (OHAM) is applied to non-linear ODE (11)-(13) with the boundary conditions (14) and (15) with the following assumptions:

$$f = f_0 + p f_1 + p^2 f_2, \quad g = g_0 + p g_1 + p^2 g_2, \quad \theta = \theta_0 + p\theta_1 + p^2 \theta_2$$

$$\mathcal{H}_1(p) = pC_1 + p^2C_2, \quad \mathcal{H}_2(p) = pC_3 + p^2C_4, \quad \mathcal{H}_3(p) = pC_5 + p^2C_6$$

where $p \in [0,1]$ is an embedding parameter, $\mathcal{H}_i(p)$ – a non-zero auxiliary function, and C_i – the constants.

$$\mathcal{L}_f = f'' + f' \quad \text{and} \quad \mathcal{N}_f = 2f''' + \left(\frac{A_1}{A_4}\right)\left[2ff'' - f'^2 + g^2\right] - \left(\frac{A_5}{A_4}\right)\frac{\text{M}}{1+m^2}(f' - mg) - \\ -\lambda f' - f'' - f'$$

$$\mathcal{L}_g = g' + g \quad \text{and} \quad \mathcal{N}_g = 2g'' + \left(\frac{A_1}{A_4}\right)\left[2fg' - 2f'g\right] - \left(\frac{A_5}{A_4}\right)\frac{\text{M}}{1+m^2}(mf' + g) - \lambda g - g - g'$$

$$\mathcal{L}_\theta = \theta' + \theta \quad \text{and} \quad \mathcal{N}_\theta = \left(1 + \frac{4R_d}{3}\right)\theta'' + \Pr\left(\frac{A_2}{A_3}\right)f\theta' + \Pr\text{Ec}\left(\frac{A_4}{A_3}\right)\left(\frac{6}{\text{Re}}f'^2 + f''^2\right) + \\ + \Pr\text{Ec}\,\text{M}\left(\frac{A_5}{A_3}\right)\left[f'^2 + g^2\right] - \theta - \theta'$$

where $\mathcal{L}_f, \mathcal{L}_g, \mathcal{L}_\theta$ are linear operators, $\mathcal{N}_f, \mathcal{N}_g, \mathcal{N}_\theta$ are non-linear operators, Therefore the OHAM family equations are:

$$(1-p)\left[f'' + f'\right] = \mathcal{H}_1(p)\left\{2f''' + \left(\frac{A_1}{A_4}\right)\left[2ff'' - f'^2 + g^2\right] - \left(\frac{A_5}{A_4}\right)\frac{\text{M}}{1+m^2}(f' - mg) - \lambda f'\right\}$$

$$(1-p)\left[g - g'\right] = \mathcal{H}_2(p)\left\{2g'' + \left(\frac{A_1}{A_4}\right)\left[2fg' - 2f'g\right] - \left(\frac{A_5}{A_4}\right)\frac{\text{M}}{1+m^2}(mf' + g) - \lambda g\right\}$$

$$(1-p)\left[\theta - \theta'\right] = \mathcal{H}_3(p)\left\{\begin{aligned}&\left(1 + \frac{4R_d}{3}\right)\theta'' + \Pr\left(\frac{A_2}{A_3}\right)f\theta' + \Pr\text{Ec}\left(\frac{A_4}{A_3}\right)\left(\frac{6}{\text{Re}}f'^2 + f''^2\right) + \\ &\qquad + \Pr\text{Ec}\,\text{M}\left(\frac{A_5}{A_3}\right)\left[f'^2 + g^2\right]\end{aligned}\right\}$$

Collecting the same powers of p, and equating each coefficient of p to zero, we obtain a set of differential equations with the associated boundary conditions. Solving differential equations with the boundary conditions, the general solution of (11)-(13) can be determined as folows.

– Zero order equations p^0:

$$f_0'' + f_0' = 0, \quad f_0(0) = 0, \quad f_0'(0) = 0 \tag{16}$$

$$g_0' + g_0 = 0, \quad g_0(0) = 1 \tag{17}$$

$$\theta_0' + \theta_0 = 0, \quad \theta_0(0) = 1 \tag{18}$$

– First order equation p^1:

$$f_1'' + f_1' = f_0'' + f_0' + C_1\left[2f_0''' + \left(\frac{A_1}{A_4}\right)\left(2f_0 f_0'' - f_0'^2 + g_0^2\right) - \left(\frac{A_5}{A_4}\right)\frac{\mathrm{M}}{1+m^2}\left(f_0' - mg_0\right) - \lambda f_0'\right]$$
$$\text{with}\quad f_1(0)=0,\ f_1'(0)=0 \tag{19}$$

$$g_1' + g_1 = g_0' + g_0 + C_3\left[2g_0'' + \left(\frac{A_1}{A_4}\right)\left(2f_0 g_0' - 2f_0' g_0\right) - \left(\frac{A_5}{A_4}\right)\frac{\mathrm{M}}{1+m^2}\left(mf_0' + g_0\right) - \lambda g_0\right]$$
$$\text{with}\quad g_1(0)=0 \tag{20}$$

$$\theta_1' + \theta_1 = \theta_0' + \theta_0 +$$
$$+C_5\left[\left(1+\frac{4R_d}{3}\right)\theta_0'' + \mathrm{Pr}\left(\frac{A_2}{A_3}\right)f_0\theta_0' + \mathrm{Pr\,Ec}\left(\frac{A_4}{A_3}\right)\left(\frac{6}{\mathrm{Re}}f_0'^2 + f_0''^2\right) + \mathrm{Pr\,Ec\,M}\left(\frac{A_5}{A_3}\right)\left(f_0'^2 + g_0^2\right)\right]$$
$$\text{with}\quad \theta_1(0)=0 \tag{21}$$

– Second order equation p^2:

$$f_2'' + f_2' = f_1'' + f_1' +$$
$$+C_1\left[2f_1''' + \left(\frac{A_1}{A_4}\right)\left(2f_0 f_1'' + 2f_1 f_0'' - 2f_0' f_1' + 2g_0 g_1\right) - \left(\frac{A_5}{A_4}\right)\frac{\mathrm{M}}{1+m^2}\left(f_1' - mg_1\right) - \lambda f_1'\right] +$$
$$+C_2\left[2f_0''' + \left(\frac{A_1}{A_4}\right)\left(2f_0 f_0'' - f_0'^2 + g_0^2\right) - \left(\frac{A_5}{A_4}\right)\frac{\mathrm{M}}{1+m^2}\left(f_0' - mg_0\right) - \lambda f_0'\right]$$
$$\text{with}\quad f_2(0)=0,\ f_2'(0)=0 \tag{22}$$

$$g_2' + g_2 = g_1' + g_1 +$$
$$+C_3\left[2g_1'' + \left(\frac{A_1}{A_4}\right)\left(2f_0 g_1' + 2f_1 g_0' - 2f_0' g_1 - 2f_1' g_0\right) - \left(\frac{A_5}{A_4}\right)\frac{\mathrm{M}}{1+m^2}\left(mf_1' + g_1\right) - \lambda g_1\right] +$$
$$+C_4\left[2g_0'' + \left(\frac{A_1}{A_4}\right)\left(2f_0 g_0' - f_0' g_0\right) - \left(\frac{A_5}{A_4}\right)\frac{\mathrm{M}}{1+m^2}\left(mf_0' + g_0\right) - \lambda g_0\right]$$
$$\text{with}\quad g_2(0)=0 \tag{23}$$

$$\theta_2' + \theta_2 = \theta_1' + \theta_1 +$$
$$C_5\left[\begin{array}{c}\left(1+\frac{4R_d}{3}\right)\theta_1'' + \mathrm{Pr}\left(\frac{A_2}{A_3}\right)\left(f_0\theta_1' + f_1\theta_0'\right) - \mathrm{Pr\,Ec}\left(\frac{A_4}{A_3}\right)\left(\frac{12}{\mathrm{Re}}f_0' f_1' + 2f_0'' f_1''\right) + \\ + \mathrm{Pr\,Ec\,M}\left(\frac{2A_5}{A_3}\right)\left(f_0' f_1' + g_0 g_1\right)\end{array}\right] +$$
$$+C_6\left[\left(1+\frac{4R_d}{3}\right)\theta_0'' + \mathrm{Pr}\left(\frac{A_2}{A_3}\right)f_0\theta_0' - \mathrm{Pr\,Ec}\left(\frac{A_4}{A_3}\right)\left(\frac{6}{\mathrm{Re}}f_0'^2 + f_0''^2\right) + \mathrm{Pr\,Ec\,M}\left(\frac{A_5}{A_3}\right)\left(f_0'^2 + g_0^2\right)\right]$$
$$\text{with}\quad \theta_2(0)=0 \tag{24}$$

Solving differential eqs. (16)-(24) with the associated boundary conditions, the general solution of (11)-(13) can be written in the form:

$$f(\eta) = f_0(\eta) + f_1(\eta) + f_2(\eta) \tag{25}$$

$$g(\eta) = g_0(\eta) + g_1(\eta) + g_2(\eta) \tag{26}$$

$$\theta(\eta) = \theta_0(\eta) + \theta_1(\eta) + \theta_2(\eta) \tag{27}$$

The residual equations for the problem obtained in the form:

$$\begin{aligned}\mathcal{R}_1(\eta, C_1, C_2) = 2f'''(\eta) + \left(\frac{A_1}{A_4}\right)\left[2f(\eta)f''(\eta) - f'^2(\eta) + g^2(\eta)\right] - \\ -\left(\frac{A_5}{A_4}\right)\frac{\mathrm{M}}{1+m^2}\left[f'(\eta) - mg(\eta)\right] - \lambda f'(\eta)\end{aligned} \tag{28}$$

$$\begin{aligned}\mathcal{R}_2(\eta, C_3, C_4) = 2g''(\eta) + \left(\frac{A_1}{A_4}\right)\left[2f(\eta)g'(\eta) - 2f'(\eta)g(\eta)\right] - \\ -\left(\frac{A_5}{A_4}\right)\frac{\mathrm{M}}{1+m^2}\left[m f'(\eta) + g(\eta)\right] - \lambda g(\eta)\end{aligned} \tag{29}$$

$$\begin{aligned}\mathcal{R}_3(\eta, C_5, C_6) = \left(1 + \frac{4R_d}{3}\right)\theta''(\eta) + \mathrm{Pr}\left(\frac{A_2}{A_3}\right)f(\eta)\theta(\eta) - \\ -\mathrm{Pr\,Ec}\left(\frac{A_4}{A_3}\right)\left[\frac{6}{\mathrm{Re}}f'^2(\eta) + f''^2(\eta)\right] + \mathrm{Pr\,Ec}\,M\left(\frac{A_5}{A_3}\right)\left[f'^2(\eta) + g(\eta)^2\right]\end{aligned} \tag{30}$$

The optimal unknown constants C_1, C_2, C_3, C_4, C_5, and C_6 can be obtained from the conditions:

$$\frac{\partial J_1}{\partial C_1} = \frac{\partial J_1}{\partial C_2} = \frac{\partial J_2}{\partial C_3} = \frac{\partial J_2}{\partial C_4} = \frac{\partial J_3}{\partial C_5} = \frac{\partial J_3}{\partial C_6} = 0$$

where

$$J_1 = \int_0^\infty \mathcal{R}_1^2(\eta, C_1, C_2)\,\mathrm{d}\eta, \quad J_2 = \int_0^\infty \mathcal{R}_2^2(\eta, C_3, C_4)\,\mathrm{d}\eta, \quad \text{and} \quad J_3 = \int_0^\infty \mathcal{R}_3^2(\eta, C_5, C_6)\,\mathrm{d}\eta \tag{31}$$

The physical quantities of interest are the local friction coefficients, C_f and C_g, and the local Nusselt number. Physically, C_f and C_g represent the dimensionless surface shear stresses, Nusselt number define the dimensionless heat transfer rate.

$$\begin{gathered}C_f = \frac{\mu_{\mathrm{nf}}}{\rho_{\mathrm{f}}(r\grave{\mathrm{U}})^2}\left[\frac{\partial u}{\partial z}\right]_{z=0}, \\ C_g = \frac{\mu_{\mathrm{nf}}}{\rho_{\mathrm{f}}(r\grave{\mathrm{U}})^2}\left[\frac{\partial v}{\partial z}\right]_{z=0}, \quad \mathrm{Nu} = \frac{1}{k_{\mathrm{f}}(T_{\mathrm{w}} - T_\infty)}\left[q_r - k_{\mathrm{nf}}\frac{\partial T}{\partial z}\right]_{z=0}\end{gathered} \tag{32}$$

The final dimensionless forms are:

$$\sqrt{\mathrm{Re}}\,C_f = A_4 f''(0),$$
$$\sqrt{\mathrm{Re}}\,C_g = A_4 g'(0), \quad \frac{\mathrm{Nu}}{\sqrt{\mathrm{Re}}} = -A_3\left(1+\frac{4R_d}{3}\right)\theta'(0) \tag{33}$$

In order to check the accuracy of the OHAM procedure used, a comparison of the velocity gradient and the temperature gradient at the disk surface at ϕ = 0.005, Pr = 6.2, Re = 1, Ec = 0.1, and $R_d = m = \lambda = 1$ are made with a numerical solution obtained by using built in function NDSolve in MATHEMATICA program. The results are tabulated in tab. 2. We note that there is a good agreement with these approaches and thus verifies the accuracy of the method used.

Table 2. Values of the velocity gradient and the temperature gradient on the surface at ϕ = 0.05, Pr = 6.2, Re = 1, Ec = 0.1, and $R_d = m = \lambda = 1$

	OHAM			Numerical		
M	$f''(0)$	$g'(0)$	$\theta'(0)$	$f''(0)$	$g'(0)$	$\theta'(0)$
0.00	0.24175	–0.76632	–0.270439	0.24175	–0.76632	–0.26822
0.50	0.28047	–0.84594	–0.189241	0.28047	–0.84594	–0.188055
1.00	0.31505	–0.91831	–0.114821	0.31505	–0.91831	–0.113994

Results and discussion

Analytical solutions are obtained for the radial and transversal velocities and the temperature of the viscous dissipation nanofluid boundary-layer over a rotating disk subjected to magnetic field with hall current and thermal radiation as external forces. Due to similarity solutions, the nanoparticles concentration, ϕ, Hartmann number, M, Hall current parameter, m , porosity parameter, λ, Eckert number, Reynolds number, and Radiation parameter, R_d have appeared through the non-linear governing system of equations. The effects of these parameters on the non-dimensional velocities and temperature are shown in figs. (2)-(15).

The study considered two types of nanoparticles CuO the results of which are plotted in solid lines and Al_2O_3 the results of which are plotted in dashed lines. On the other hand, the effects of all embedded parameters on the surface shear stress and the rate of heat transfer are listed in tabs. 3-6.

The effect of nanoparticles concentration

Figures 2-4 show the effect of the nanoparticles concentration on the radial velocity, transverse velocity, and the fluid temperature. It is clear that the increase of nanoparticles concentration increases the radial velocity and the temperature of the boundary-layer over the rotated disk. In contrast, there is no considerable effect of the nanoparticles concentration on the transversal velocity as shown in fig. 2.

Table 3 presents the velocities gradient and temperature gradient over the disk surface and the corresponding values of surface skin friction and the rate of heat transfer for different concentrations of the nanoparticles. It is clear that the increasing of the concentration increases the skin friction over the disk surface in both of radial and transversal directions. Moreover, one can observe that the rate of heat transfer is reduced by the increase of concentration. Such behavior indicates that the viscous dissipation has a direct effect on the temperature gradient, such that the presence of kinematic viscosity of the nanoparticles decreases the temperature gradient at the surface.

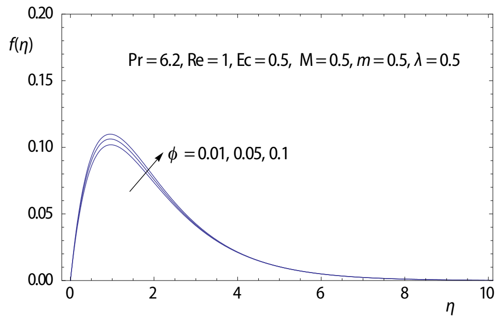

Figure 2. Radial velocity profile with increasing nanoparticles concentration

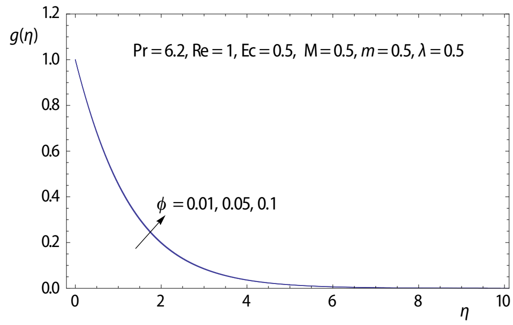

Figure 3. Transversal velocity profile with increasing nanoparticles concentration

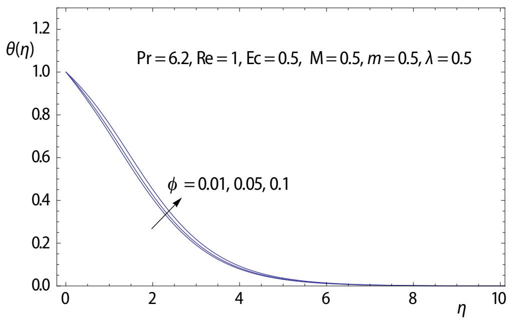

Figure 4. Temperature profile with increasing nanoparticles concentration

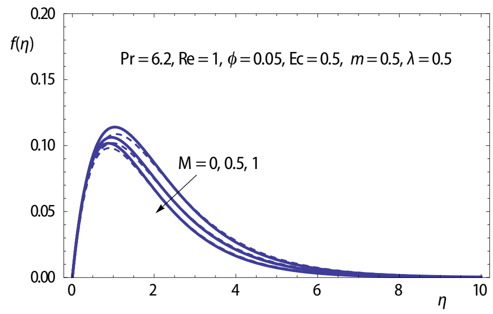

Figure 5. Radial velocity profile with increasing Hartmann number

Table 3. Values of the velocity gradient and the temperature gradient on the surface at Pr = 6.2, Re = 1, Ec = R_d = M = m = λ = 0.5

		CuO-water					
		$f''(0)$	$g'(0)$	$\theta'(0)$	C_f	C_g	Nu
ϕ	0.01	0.28990	–0.74942	–0.08499	0.29728	–0.76849	0.14184
	0.05	0.30464	–0.74114	–0.08113	0.34632	–0.84254	0.13611
	0.10	0.31529	–0.72873	–0.07536	0.41030	–0.94833	0.12725
		Al_2O_3-water					
		$f''(0)$	$g'(0)$	$\theta'(0)$	C_f	C_g	Nu
ϕ	0.01	0.28550	–0.74695	–0.08435	0.29276	–0.76596	0.14149
	0.05	0.28477	–0.72950	–0.07866	0.32373	–0.82931	0.13541
	0.10	0.28029	–0.70749	–0.07192	0.36475	–0.92069	0.12783

The effect of magnetic field (Joule heating)

The effect of magnetic field appears in this study through the Hartmann number. The effects of this number on the boundary-layer velocities are shown in figs. 5 and 6 such that one can observe that the increase of Hartmann number decreases the velocity in both of radial and transversal directions. Moreover, the profile of the radial velocity refers to an increasing of the CuO-water velocity near the disk surface in comparison to that of Al_2O_3-water but the opposite is true for the transversal velocity.

On the other hand, the impact of Joule heat on the thermal boundary-layer appears through the Hartmann number. It is clear from fig. 7 that the presence of Joule heating increase the nanoparticles motion which, respectively, increase the boundary-layer temperature.

The effect of Hall current.

Figures 8-10 show the effects of Hall current on the boundary-layer velocities and temperature. It is clear that the increase of the Hall current parameter, m, increases the radial velocity but decreases the transversal velocity and temperature. Moreover, one can observe that the impact of this parameter is clear and effective on the radial velocity compared to the transversal velocity. Figure 9 shows that the impact of Hall parameter on Al_2O_3-water is higher than that on CuO-water.

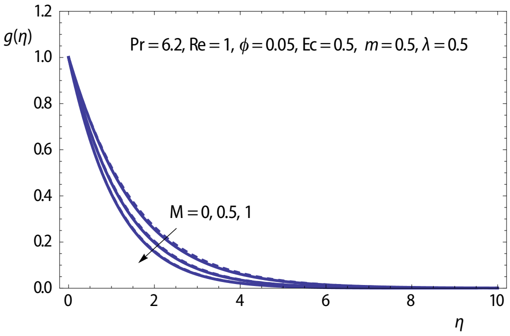

Figure 6. Transversal velocity profile with increasing Hartmann number.

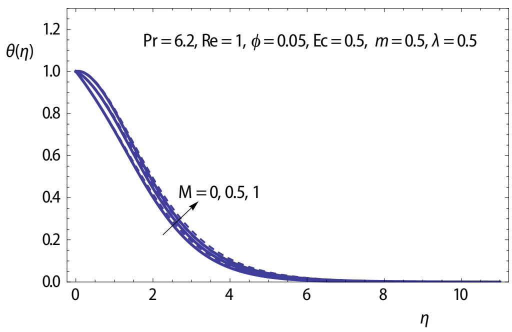

Figure 7. Temperature profile with increasing Hartmann number.

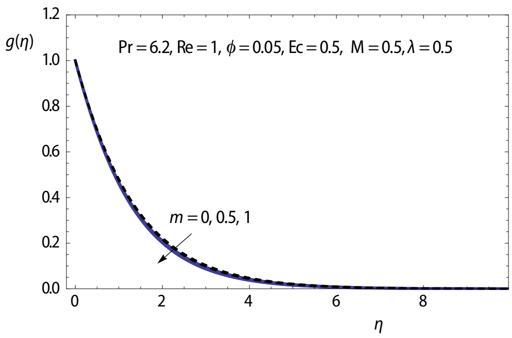

Figure 8. Radial velocity profile with increasing Hall current parameter

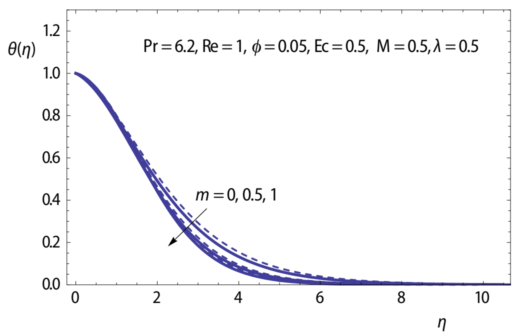

Figure 9. Transversal velocity profile with increasing Hall current parameter

Tables 4 and 5 show the effect of magnetic field with/without Hall current on the skin friction and the rate of heat transfer, it is clear that the presence of magnetic field without Hall current decreases the radial velocity gradient and increases the transversal velocity and temperature gradient. Such behavior results in decreasing the skin friction in the radial direction, increasing the skin friction in the transversal direction and increasing the rate of heat transfer. The skin friction along the transversal direction and the rate of heat transfer have no change in behavior in the presence of magnetic field with Hall current but the main change appears in the radial direction such that the value of skin friction in this direction increases with the increase of Hartmann number.

Table 4. Values of the velocity gradient and the temperature gradient on the surface at Pr = 6.2, Re = 1, ϕ = 0.05, R_d = Ec = m = λ = 0.5

	CuO-water						
m	M	$f''(0)$	$g'(0)$	$\theta'(0)$	C_f	C_g	Nu
0	0.00	0.29667	–0.61692	–0.22819	0.33726	–0.70133	0.38281
	0.50	0.24915	–0.74264	–0.08973	0.28324	–0.84425	0.15053
	1.00	0.21642	–0.85899	0.05666	0.24603	–0.97652	–0.09505
0.5	0.00	0.29667	–0.61692	–0.22819	0.33726	–0.70133	0.38281
	0.50	0.30464	–0.74114	–0.08113	0.34633	–0.84254	0.13611
	1.00	0.31565	–0.84924	0.04186	0.35884	–0.96544	–0.07023
	Al_2O_3-water						
m	M	$f''(0)$	$g'(0)$	$\theta'(0)$	C_f	C_g	Nu
0.5	0.00	0.27453	–0.60162	–0.23038	0.31209	–0.68393	0.39660
	0.50	0.28477	–0.72950	–0.07866	0.32374	–0.82931	0.13541
	1.00	0.29761	–0.83975	0.04634	0.33833	–0.95465	–0.07978

Table 5. Values of the velocity gradient and the temperature gradient on the surface at Pr = 6.2, Re = 1, ϕ = 0.05, R_d = Ec = m = 0.5

	CuO-water						
		$f''(0)$	$g'(0)$	$\theta'(0)$	C_f	C_g	Nu
λ	0.00	0.37016	–0.60062	0.02537	0.42080	–0.68279	–0.04255
	0.50	0.30464	–0.74114	–0.08113	0.34633	–0.84254	0.13611
	1.00	0.25999	–0.87389	–0.10570	0.29557	–0.99346	0.17732
	Al_2O_3-water						
		$f''(0)$	$g'(0)$	$\theta'(0)$	C_f	C_g	Nu
λ	0.00	0.35074	–0.58338	0.02874	0.39873	–0.66320	–0.04947
	0.50	0.28477	–0.72950	–0.07866	0.32374	–0.82931	0.13541
	1.00	0.24128	–0.86600	–0.09909	0.27429	–0.98449	0.17058

The effect of porous medium

The effect of the permeable medium considered in the study is taken from the porosity parameter. Figures 11-13 show the impact of λ on the velocities and temperature of the boundary-layer. It is clear that the velocities in the both direction decrees by the increase of λ. On the other hand, considering λ increases the temperature. One can also observe that the effect of this parameter on the temperature is clear in the case of Al_2O_3-water more than the case of CuO-water.

Rate of heat transfer and the transverse skin friction both increase by the increase of λ as shown in tab. 5 and the opposite is true for the radial skin friction.

The effect of viscous dissipation and thermal radiation

Figure 14 show the effect of Eckert number and radiation parameter on the boundary-layer temperature. Eckert number is the ratio between the flow's kinetic energy and the enthalpy. According to the profile of the temperature, the increase of Eckert number increases the kinetic energy that consequently increases the temperature. The same effect appears in fig. 15 for the radiation parameter, R_d, such that increasing the R_d decreases the mean absorption coefficient, which consequently increases the temperature.

Table 6 shows the effect of Eckert number and radiation parameter on the temperature gradient. It is clear that the temperature gradient decreases in the presence of any of them.

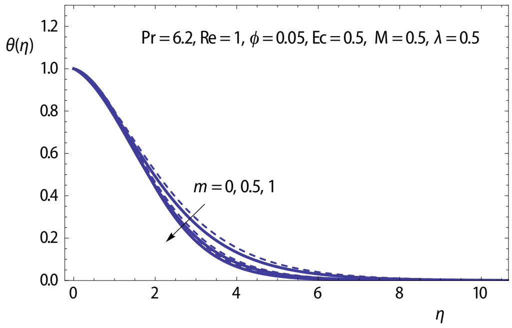

Figure 10. Temperature profile with increasing Hall current parameter

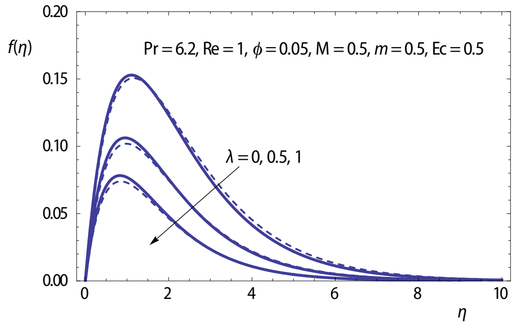

Figure 11. Radial velocity profile with increasing porosity parameter

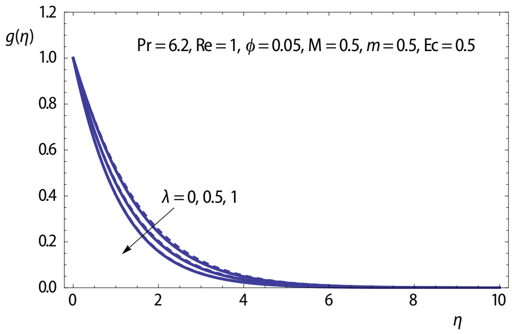

Figure 12. Transversal velocity profile with increasing porosity parameter

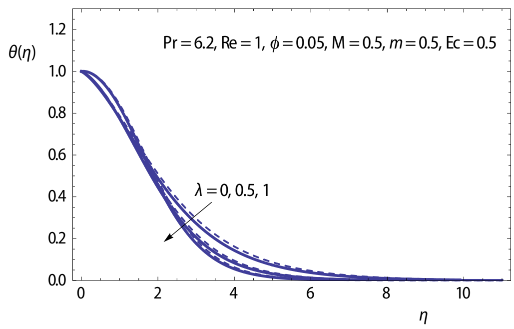

Figure 13. Temperature profile with increasing porosity parameter

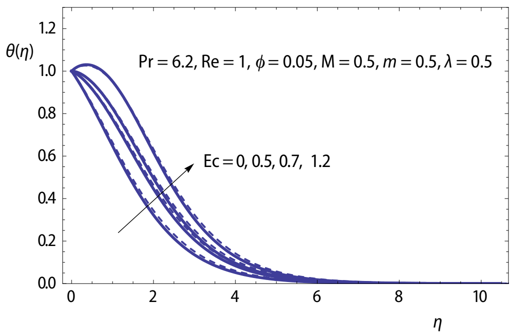

Figure 14. Temperature profile with increasing Eckert number

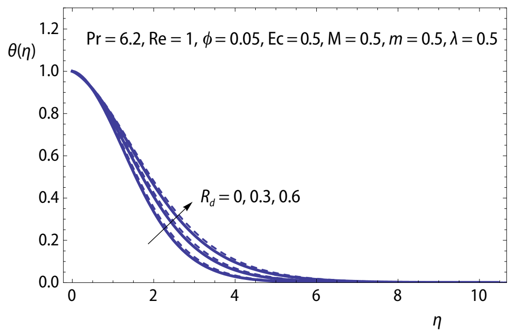

Figure 15. Temperature profile with increasing radiation parameter

Conclusions

In this paper, we have studied analytically the magnetic field with Hall current and Joule heating, viscous dissipation effects on flow and heat transfer over a rotating disk into porous medium consists of water with two types suspended nanoparticles. The following results are obtained.

Table 6. Values of the velocity gradient and the temperature gradient on the surface at Pr = 6.2, Re = 1, ϕ = 0.05, λ = M = m = 0.5

CuO-water					
Ec	$\theta'(0)$	Nu	Rd	$\theta'(0)$	Nu
0.00	–0.27282	0.45768	0.00	–0.02689	0.02706
0.50	–0.08113	0.13611	0.60	–0.06805	0.09589
1.20	0.18723	–0.31410	1.20	–0.08543	0.15478
Al_2O_3-water					
Ec	$\theta'(0)$	Nu	Rd	$\theta'(0)$	Nu
0.00	–0.25431	0.43780	0.00	–0.02622	0.02709
0.50	–0.07866	0.13541	0.50	–0.06604	0.11368
1.20	0.16726	–0.28794	1.00	–0.08279	0.19953

- From the profiles showed the radial velocity of the flow over the rotation disk increases in the presence of Hall current and the increasing of nanoparticles concentration. While the opposite effect appears in the presence of magnetic field and porosity parameters.
- The transversal velocity of the flow over the rotation disk decreases in the presence of Hall current, magnetic and porosity parameters.
- Boundary-layer temperature increases with the increase of nanoparticles concentration, porosity parameter, Eckert number, and radiation parameter.
- Rate of heat transfer over the disk increases in the presence of magnetic field and decreases with the increase of Hall current.
- The effect of Hall current is clearer and bigger on the radial skin friction than that on the transverse skin friction.

References

[1] Von Karman, T., Classical Problem of Rotating Disk, *Transfer ASME, Vol. 61,* 1939
[2] Cochran, W. G., The Flow Due to a Rotating Disk, *Camb. Philos. Soc. 30* (1934), 3, pp. 365-375
[3] Benton, E. R., On the Flow Due to a Rotating Disk, *J. Fluid Mech*., *24* (1966), 4, pp. 781-800
[4] Rogers, M. G., Lance, G. N., The Rotationally Symmetric Flow of a Viscous Fluid in Presence of Infinite Rotating Disk, *J. Fluid Mech., 7* (1960), 4, pp. 617-631
[5] Erdogan, M. E., Unsteady Flow of a Viscous Fluid Due to Non-Coaxial Rotations of a Disk and a Fluid at Infinity, *International Journal of Non-Linear Mechanics, 32* (1997), 2, pp. 285-290
[6] Turkyilmazoglu, M., Nanofluid Flow and Heat Transfer Due to a Rotating Disk, *Computers & Fluids, 94* (2014), May, pp. 139-146
[7] Sheikholeslami, M., *et al.*, Nanofluid Flow and Heat Transfer in a Rotating System in the Presence of a Magnetic Field, *Journal of Molecular Liquids, 190* (2014), Feb., pp.112-120
[8] Elbashbeshy, E. M. A., Emam, T. G., Effects of Thermal Radiation and Heat Transfer over an Unsteady Stretching Surface Embedded in a Porous Medium in the Presence of Heat Source or Sink, *Thermal Science*, *15* (2013), 2, pp. 477-485
[9] Hayat, T., *et al.*, Magnetohydrodynamic (MHD) Flow of Cu-Water Nanofluid Due to a Rotating Disk with Partial Slip, *AIP Advances, 5* (2015), 6, 067169
[10] Choi, S. U. S., Eastman, J. A., Enhancing Thermal Conductivity of Fluids with Nanoparticles, *ASME International Mechanical Engineering Congress and Exposition, 66* (1995), Oct., pp. 99-105
[11] Liron, N., Wilhelm, H. E., Integration of the Magneto-Hydrodynamic Boundary Layer Equations by Meksyn's Method, *J. Appl. Math. Mech*., (*ZAMM*) *54* (1974), 1, pp. 27-37
[12] Elbashbeshy, E. M. A., *et al.*, The Effect of Thermal Radiation and Heat Generation on the Mechanical Properties of Unsteady Continuous Moving Cylinder in a Nanofluid in the Presence of Suction or Injection, *Thermal Science*, *19* (2015), 5, pp. 1591-1601
[13] Elbashbeshy, E. M. A., *et al.*, Flow and Heat Transfer over a Moving Surface with Non-Linear Velocity and Variable Thickness in a Nanofluid in the Presence of Thermal Radiation, *Can. J. Phys*., *92* (2014), 2, pp. 124-130

[14] Makinde, O. D., *et al.,* MHD Flow of a Variable Viscosity Nanofluid over a Radially Stretching Convective Surface with Radiative Heat, *Journal of Molecular Liquids*, *219* (2016), July, pp. 624-630
[15] Khamis, S., *et al.,* Unsteady Flow of Variable Viscosity Cu-Water and Al_2O_3-Water Nanofluids in a Porous Pipe with Buoyancy Force, *International Journal of Numerical Methods in Heat and Fluid Flow*, 25 (2015), 7, pp. 1638-1657
[16] Makinde, O. D., Effects of Viscous Dissipation and Newtonian Heating on Boundary Layer Flow of Nanofluids over a Flat Plate, *International Journal of Numerical Methods for Heat and Fluid flow*, *23* (2013), 8, pp. 1291-1303
[17] Motsumi, T. G., Makinde, O. D., Effects of Thermal Radiation and Viscous Dissipation on Boundary Layer Flow of Nanofluids over a Permeable Moving Flat Plate, *Physical Scripta*, *86* (2012), 045003
[18] Rashidi, M. M., *et al.*, Entropy Generation in Steady MHD Flow Due to a Rotating Porous Disk in a Nanofluid, *Int. J. Heat Mass Transfer, 62* (2013), July, pp. 515-525
[19] Chauhan, D. S., Rastogi, P., Heat Transfer Effects on Rotating MHD Couette Flow in a Channel Partially Filled by a Porous Medium with Hall Current, *Journal of Applied Science and Engineering*, *15* (2012), 3, pp. 281-290
[20] Babaelahi, M., *et al.*, Viscoelastic MHD Flow Boundary Layer over a Stretching Surface with Viscous and Ohmic Dissipations, *Meccanica, 45* (2010), 6, pp. 817-827
[21] Sheikholeslami, M., *et al.*, Numerical Simulation of MHD Nanofluid Flow and Heat Transfer Considering Viscous Dissipation, *International Journal of Heat and Mass Transfer*, *79* (2014), Dec., pp. 212-222
[22] Abdel-Wahed, M. S., *et al.*, Flow and Heat Transfer over a Moving Surface with Non-Linear Velocity and Variable Thickness in a Nanofluid in the Presence of Brownian Motion, *Applied Mathematics and Computation*, *254* (2015), Mar., pp. 49-62
[23] Liao, S., An Optimal Homotopy-Analysis Approaches for Strongly Nonlinear Differential Equations, *Commun Nonlinear Sci. Numer. Simulat.*, *15* (2010), 8, pp. 2003-2016

Paper submitted: March 12, 2016
Paper revised: August 8, 2016
Paper accepted: August 14, 2016